

Efficient Neural Clause-Selection Reinforcement

Martin Suda^[0000–0003–0989–5800]

Czech Technical University in Prague, Czech Republic
martin.suda@cvut.cz

Abstract. Clause selection is arguably the most important choice point in saturation-based theorem proving. Framing it as a reinforcement learning (RL) task is a way to challenge the human-designed heuristics of state-of-the-art provers and to instead automatically evolve—just from prover experiences—their potentially optimal replacement.

In this work, we present a neural network architecture for scoring clauses for clause selection that is powerful yet efficient to evaluate. Following RL principles to make design decisions, we integrate the network into the VAMPIRE theorem prover and train it from successful proof attempts. An experiment on the diverse TPTP benchmark finds the neurally guided prover improve over a baseline strategy, from which it initially learns—in terms of the number of in-training-unseen problems solved under a practically relevant, short CPU instruction limit—by 20%.

Keywords: Saturation-based Theorem Proving · Clause Selection · Deep Reinforcement Learning

1 Introduction

Reinforcement learning (RL) [39] is a machine learning (ML) paradigm in which an agent learns to make sequential decisions by interacting with an environment and maximizing cumulative rewards. The impressive successes of RL in board games [32] or on the Atari benchmark [25] motivate researchers to apply RL to their own domains of interest. It is exciting to have an unsupervised method search for a decision strategy unbiased by our human preconceptions, since this intuitively increases the chances of discovering brand new approaches.

In automatic theorem proving (ATP), we have seen the Monte-Carlo tree search [18] guide a connection tableaux prover [17, 43] or, more recently, proximal policy optimization [29] applied to dynamically pick clause selection queues [31] in a saturation-based prover [24]. Despite these achievements, substantial performance improvements over the state of the art have so far only been reported for systems employing the more straightforward supervised learning methods [15, 34, 7]. Moreover, the published results predominantly focus on problem sets with a common origin and encoding, such as the Mizar40 set [16], arguably more amenable to ML techniques than the canonical theorem proving benchmark used by the CASC [37] competition, the TPTP library [38].

In this work, we apply a policy gradient RL method [42] to train a neural-network-based clause selection heuristic for the ATP VAMPIRE [19]. As a highly

optimized system, VAMPIRE can generate and evaluate thousands to millions of clauses within seconds. Not to impede the prover’s high inference speed with the new guidance, we design a neural network architecture that is powerful yet efficient to evaluate (Sect. 4). Analyzing clause selection through the lens of RL (Sect. 3), we propose a new learning operator for iteratively improving the network’s performance from successful proof attempts (Sect.3.1). We adopt a rather counterintuitive idea in this context and reject the concept of a state to make our agent govern a single, standalone clause selection queue (Sect. 5).

Even on the diverse TPTP benchmark, our new system is able to improve over VAMPIRE’s default strategy, from which it initially learns, by 20%. This is done in a sanitized setting (using a train/test split) and for practically relevant proving times of approximately 10s per problem. Moreover, we find that the trained neurally-guided VAMPIRE solves more than 100 problems of rating 1.0, roughly half of which have not been recorded as proven by any system to date. Improvements of this magnitude are exceptionally rare in the literature, particularly in terms of solving previously unrecorded problems.

After the experiments (Sect. 6), the paper reviews related work (Sect. 7) and ends with a conclusion with outlooks for future work (Sect. 8).

2 Background

In this section, we review the basic concepts related to saturation-based theorem proving and reinforcement learning.

2.1 Saturation-Based Theorem Proving

The most successful provers for first-order logic such as E [30], iProver [8], SPASS [41] or Vampire [19], are *refutational*, based on *saturation*. The former means they aim for a proof by contradiction: Given an input problem P consisting of a set of axioms \mathcal{A}_P and a conjecture G_P , they start by negating the conjecture and computing an equisatisfiable clause normal form $CNF(\mathcal{A}_P \cup \{\neg G_P\}) = C_P$ and then set out to show that this set of clauses C_P is unsatisfiable.

During the saturation process which follows, the provers strive to compute a closure of these clauses with respect to a selected inference system \mathcal{I} . Saturation is most often implemented by a *given-clause algorithm*, which keeps track of inferences by working with two sets of clauses: the *active* set \mathcal{A} (initially empty) and the *passive* set \mathcal{P} (initialized with the input clauses). It maintains an invariant that every inference with all premises in \mathcal{A} has already been performed. Iteratively, a clause C is *selected* from \mathcal{P} , moved to \mathcal{A} (and thus *activated*), and all inferences with at least one premise being C and others coming from \mathcal{A} are computed and their conclusions are added to \mathcal{P} .

There are several variants of the given-clause algorithm [28]. They mostly differ in how they deal with simplifications and redundancy elimination, a crucial topic for performance, but not immediately relevant for our exposition.

Clause Selection: Heuristics are employed to decide, in each iteration, which clause from \mathcal{P} to select next for activation. An imagined perfect heuristic would only select clauses from the yet-to-be-discovered proof (all other selections constitute in retrospect a wasted effort). Such an ideal, however, must be intractable to compute as it would essentially eliminate search from the proving task. In practice, it is thus important with clause selection to carefully trade between the quality of the decisions and the computational effort spent on making them.

Provers typically implement the passive clause container as a collection of *priority queues*, each queue representing \mathcal{P} sorted by a distinct *clause evaluation function* (CEF). The two most commonly used CEFs are *age* and *weight*, the first encoding a preference for older clauses and the second a preference for clauses with fewer symbols. The prover then alternates between the queues under a specified *ratio* (called the pick-given ratio in OTTER’s manual [23]) and selects the best clause from the current queue in each iteration.

2.2 Reinforcement Learning

Reinforcement Learning (RL) is an optimization framework that enables an *agent* to learn an optimal decision-making *policy* through trial and error by interacting with an *environment* and receiving feedback in the form of a *reward*. In what follows, we quickly summarize the main RL concepts; we refer the interested reader to a standard textbook [39] for a thorough formal treatment.

We focus here on a conceptualization of RL via finite Markov Decision Processes (MPDs), in which time is modeled as passing in discrete steps. In each step, the agent reflects on the current *state* s of the environment and correspondingly chooses one of possible *actions* to take. One time step later, in part as a consequence of the chosen action a , the agent receives a numerical reward r and finds itself in a new state s' . This transition (including the reward) is in general stochastic, specified by a probability distribution $p(s', r | s, a)$.

A policy is a mapping from states to probabilities of selecting each of the available actions, denoted $\pi(a | s)$. A *value* $v(s)_\pi$ of a state s under a policy π is the expected *return*, i.e., the reward accumulated (optionally under discounting) over a trajectory starting at s and following π . RL optimizes a policy to maximize the expected return (from any state). Thus, aiming for a high reward in the distance can be more important than collecting mediocre rewards immediately.

3 Clause Selection Reinforcement

Let us consider a standard clause selection heuristic like the age-weight alternation, as if driven by an RL agent. Such an agent monitors the prover’s state and chooses appropriate actions to reach the goal of deriving the empty clause, ideally in the smallest number of steps possible. Our idea is to use this perspective to guide our decisions about the design of a new agent for the task, backed by a neural network and learned through reinforcement from proving experiences.

One of our aims is to make sure that the new design accommodates the old heuristic as an attainable point in the space of possible solutions. This provides for a useful sanity check, as well as a good promise for the potential to go beyond the state of the art, at least as long as the computational overhead stays relatively low and there is anything new and relevant to learn from the data.

State. The state of a clause selection heuristic naturally decomposes into two conceptual parts: a *static* one, the problem P given as input, and an *evolving* one, any information influencing which of the clauses in the current passive set should be selected next in order to solve P (i.e., show that C_P is unsatisfiable).

Surprisingly, state-of-the-art provers, backed by decades of research and experimentation, mostly ignore the evolving state for clause selection.¹ Except possibly for a few bits to remember which queue to select the next clause from,² the effective state is blank and each selection aims greedily at the best available clause. This could be mostly for efficiency reasons; after all, if a clause evaluation function was to change from state to state, we could no longer cheaply keep the passive set represented as an ordered queue.

Speculations aside, we take this observation as an indication that proof planning is not a viable approach to general-purpose saturation-based proving (in its contemporary form) and bake the assumption of a single-state—effectively “stateless”—environment into our design.

Actions. At each iteration of the saturation loop, clause selection picks one of the clauses in the passive set for activation. We therefore equate the set of available actions (at a given moment) with the current content of the passive set.

Reward. An essential facet of any RL environment is the reward. Since it is a priori not clear during saturation which clauses will eventually constitute the discovered proof, the ideal, most faithful-to-reality environment should intuitively only assign a non-zero reward to the final, empty-clause-deriving step. However, an agent would only have a chance to reasonably learn from such a sparse reward through massive exploration (trial and error) and value bootstrapping.³ As we already decided not to work with states, such avenue is effectively ruled out.

We instead follow most other ML-based approaches to clause selection guidance [6, 1, 24] in this regard, learn from the successful proof attempts only, and assign a reward to actions retrospectively, based on which clauses end up in the discovered proof. In more detail, at every step, each passive clause C that is in fact a future proof clause gets a reward $r_C = 1$ and the remaining, non-proof clauses receive $r_C = 0$. As detailed later (cf. Sect. 3.1 below), we also subject

¹ Static state enters the picture when selecting proving strategies or strategy schedules.

² Although, within the RL framework, deterministic queue alternation might best be seen as a poor man’s implementation of a probabilistic choice.

³ Bootstrapping in RL means updating estimates based on other estimates instead of waiting for the full return and represents a solution to the *credit assignment problem*, the challenge of determining which actions were responsible for a received reward.

these rewards to several forms of scaling, with the intuitive idea to give each solved problem a fair share in influencing the update of the trained network.

3.1 RL-Inspired Learning Operator

Let a *trace* of a successful proof attempt on problem P_T be a tuple

$$T = (P_T, \mathcal{C}, \mathcal{C}^+, \{\mathcal{P}_i\}_{i \in I_T}),$$

where \mathcal{C} is the set of all input and derived clauses, $\mathcal{C}^+ \subseteq \mathcal{C}$ marks clauses that ended up in the found proof, and the $\mathcal{P}_i \subseteq \mathcal{C}$ are the snapshots of the content of the passive set at each iteration $i \in I_T$ of the saturation loop just before clause selection. By a *learning operator* for clause selection we mean a procedure that receives as input a set of traces \mathcal{T} and a neural network N_{θ} , described by a vector of learnable parameters θ , and updates these parameters to obtain θ' , so that $N_{\theta'}$ is now better suited for solving the problems that gave rise to \mathcal{T} and ideally also generalizes well to solve other problems.

The learning operator we describe here is derived from the REINFORCE algorithm and the accompanying policy gradient theorem [42]. This algorithm is an ideal approach for directly optimizing a policy⁴ using gradient descent. We avoid introducing the algorithm in its full generality (see [39] for more details) and instead immediately describe how it is reflected in our learning operator. We start by recalling a standard trick from deep RL and the key theorem.

Logits and Softmax. We assume our network N_{θ} produces a score $N_{\theta}(C) = l_C$, usually called the *logit*, for each available action, i.e., for each clause C from the passive set \mathcal{P} in our case. The logits are to be normalized via the softmax function to yield a probability distribution

$$\pi_C = \text{softmax}_C(\{l_D\}_{D \in \mathcal{P}}) = \frac{e^{l_C}}{\sum_{D \in \mathcal{P}} e^{l_D}}.^5$$

This allows us to construe the clauses' scores, at any given moment, as a stochastic clause selection policy. The stochastic aspect is an inherent part of the theory, but not a necessary component in an implementation (cf. Sect. 5.1).

Policy Gradient. Let $\alpha > 0$ be a learning step parameter. The key theorem behind REINFORCE tells us that in order to improve a policy in terms of the expected return, we should update the network parameters as in

$$\theta \leftarrow \theta + \alpha R_C \nabla_{\theta} \log \pi_C, \tag{1}$$

i.e., in the direction of the gradient $\nabla_{\theta} \log \pi_C$ and with a magnitude proportional to R_C , the return accrued in an episode following π which chose C at a particular step. In our stateless setup, we will be using the immediate rewards r_C instead.

⁴ Another family of approaches, the value-based methods, work by learning (to approximate) the state value function and thus rely on meaningful states.

⁵ As such, the logits are dimensionless and have only relative meaning: $l_C - l_D = d$ signifies that clause C should be e^d -times more likely to get selected than clause D .

Our Operator. Let \mathcal{T} be a set of traces and N_{θ} our network. We treat each moment in time in each of the given traces as an independent opportunity to improve the clause evaluation function that N_{θ} represents. This also includes the moments in which the prover selected a different clause than a future proof clause, for which the reward is 0, and thus strictly following (1) would lead to no nontrivial update. We instead always learn from all proof clauses that are on the passive set and average their contributions to the gradient.⁶

For every $T = (P_T, \mathcal{C}, \mathcal{C}^+, \{\mathcal{P}_i\}_{i \in I_T}) \in \mathcal{T}$ and every $i \in I_T$, we define the *good passive clauses at step i* as $\mathcal{P}_i^+ = \mathcal{P}_i \cap \mathcal{C}^+$ and the corresponding gradient contribution as

$$\delta_i^T = \text{mean}_{C \in \mathcal{P}_i^+} \nabla_{\theta} \log \pi_C.$$

Additionally, we set $\delta^T = \text{mean}_{i \in I_T} \delta_i^T$ and $\delta = \text{mean}_{T \in \mathcal{T}} \delta^T$ as the contribution of a single trace and of the whole set, resp. In experiments containing more than one trace for a single problem we insist that “all problems are equal” (not to allow the more represented ones to have more strength) and instead use:

$$\delta^P = \text{mean}_{T \in \mathcal{T}, P_T = P} \delta^T \quad \text{and} \quad \delta^{fair} = \text{mean}_{P, \exists T \in \mathcal{T}, P_T = P} \delta^P.$$

We remark that the operator can be applied to any set of traces \mathcal{T} , not just those generated by a prover guided by a clause selection driven by N_{θ} . However, the latter is the typical way of using it. Namely, to apply the operator repeatedly, building a sequence of guiding networks and trace sets $N_{\theta_1}, \mathcal{T}_1, N_{\theta_2}, \mathcal{T}_2 \dots$, where network N_{θ_j} is used to generate the traces \mathcal{T}_j for the subsequent improvement round, until an optimum performance is achieved.

4 Neural Clause Evaluation

The neural network (NN) architecture proposed in this work is designed to be general-purpose and efficient to evaluate. The first property mandates *name invariance*: we do not allow the network to base its decisions on concrete symbol names as these may change meaning from one input problem to the next.⁷

One-off GNN Invocation. Previous work has established Graph Neural Networks (GNNs) as a good basis for name invariant neural formula representations [26, 13, 1]. However, GNNs are relatively expensive to evaluate and intuitively work best when given a large formula (i.e., many clauses) to evaluate at once, so that individual constituents (sub-formulas, terms, symbols) provide sufficient context for one another [5, 9]. This becomes tricky when evaluating clauses for clause selection, as the group of newly derived clauses, which need to be evaluated after each activation, varies in size and is typically relatively small.

⁶ This is one of the aspects in which we depart from the pure RL paradigm and are choosing a pragmatic approach instead.

⁷ For instance, in the TPTP library which we target for our experiments, each individual problem comes with its own symbol signature, and any name overlap between two problems’ signatures can be considered purely coincidental.

We avoid these complications by running a GNN only once, at the beginning of the saturation process on the input problem’s CNF, and have the GNN prepare name-invariant vectorial representations (so called *embeddings*) of the signature symbols and the input clauses, to be further utilized in subsequent processing.

Generalizing Age and Weight with RvNNs. The idea is to use these embeddings to seed computations of two (independent) Recursive Neural Networks (RvNN) [20]. One RvNN starts from the input clause embeddings and unrolls along the clause derivation tree (as in [33]), the other starts from the symbol embeddings and unrolls along the clause parse tree (as in [6]). In fact, it is advantageous to treat each of these trees as a directed acyclic graph (DAG), share the common subgraphs and cache the results for the already computed subgraphs.⁸

One can think of these two RvNNs as allowing the training process to generalize and improve upon the two most commonly used standard clause evaluation functions, age and weight. Clause age is essentially the depth of the derivation tree, while weight equals the number of nodes in the parse tree. As such, they could in principle be learned even without the initial embeddings from the GNN. However, we hope that the network discovers much more powerful CEFs still.

Completing the Neural CEF. To complete the tower of NN modules and obtain a final score for a clause, we concatenate the embeddings from the two RvNNs with a vector of 12 easy-to-compute simple clause features. These features include the standard age and weight, the number of literals based on their polarity, the number of variable occurrences or the number of AVATAR [40] splits a clause depends on.⁹ The concatenated vector is then fed to a simple fully-connected NN with one hidden layer and a single clause score output.

4.1 Note on Efficient RvNNs

The general rule for making NN computation fast is to group as many operations as possible into one high-level one, which can be vectorized (such as matrix multiplication) and executed via a single (optimized) library call. This is often obvious to do with “rectangular“ or otherwise regular inputs such as images, but can be tricky with DAGs traversed by our RvNNs.

In contrast to our previous work [33, 34], we strive here to maximize such grouping by postponing node evaluations as much as possible and enqueueing the pending operations into layers based on their dependencies. The essence of the idea is captured in Fig. 1 on the example of the generalized-age (*gage*) RvNN.

To understand Fig. 1, let us first explain its context and how it is initialized. The code maintains for each clause its `height`, which the input clauses have set to 0 and the derived clauses get assigned here on line 3. The main task of the

⁸ In an ATP implementing perfect term sharing, we maintain at most one fixed-size embedding per shared subterm. This shows that the overhead of the network maintenance does not increase the prover’s asymptotic time (or space) complexity.

⁹ See Appendix A for a complete list.

```

def gage_insert(cl_num:int, inf_rule:int, parents:list[int]): 1
    level = max(base_level, 1 + max(height[p] for p in parents)) 2
    height[cl_num] = level 3
    index = level - base_level 4
    if len(todo_layers) == index: 5
        todo_layers.append([]) 6
    todo_layers[index].append((cl_num, inf_rule, parents)) 7

```

Fig. 1. Python code for inserting clause `cl_num` derived by inference rule `inf_rule` from parents `parents` for later processing by the generalized-age (`gage`) RvNN.

shown function is to insert a new clause (along with the information of how it got derived) into the buffer `todo_layers` at the lowest possible index, so that clauses at the individual layers are independent and can be evaluated together, provided the embeddings for the lower layers have already been computed.

Thus, when later evaluating the inserted clauses, this can be done in a layer-by-layer fashion, in a single bulk operation per layer. Thereupon, `base_level` is incremented by the number of the processed layers and the `todo_layers` buffer itself is cleared. This arrangement has the property that `height` of a clause does not need to change once set, and the code works both during inference, where many evaluations are triggered over time, and during training, where a maximal “compression” can be enjoyed and the `todo_layers` buffer is filled only once.¹⁰

One additional condition must, however, be met for the bulk operations to be possible, namely that there is only a single “combine” operation for our RvNN and that each node to evaluate can be represented by a fixed-size vector. In the example of our generalized-age network, we achieve this by concatenating a trainable inference rule embedding with exactly two parent embedding slots. The first slot is reserved for the embedding of the main premise and the second averages the embeddings of all the remaining premises (if present).

4.2 Architecture Details

A sketch of our architecture is shown in Fig. 2. Following it from left to right, we see how the input CNF is first turned into a graph consisting of five kinds of nodes (sort, symbol, variable, subterm, and clause nodes) and several kinds of edges. The graph is then processed by k rounds of message-passing GNN, where k is a hyper-parameter, producing embeddings for symbols and for the input clauses. The GNN is evaluated once, before saturation begins.

During saturation, the generalized-weight RvNN incrementally (on demand) produces embeddings of subterms, literals, and the derived clauses themselves, following their syntax structure. In addition to the symbol embeddings from the GNN it also uses one trainable “variable node” embedding (denoted by an empty circle in Fig. 2) to represent any variable term (i.e., we deliberately conflate

¹⁰ In our experiments, the median height of the clause derivation tree was 10.

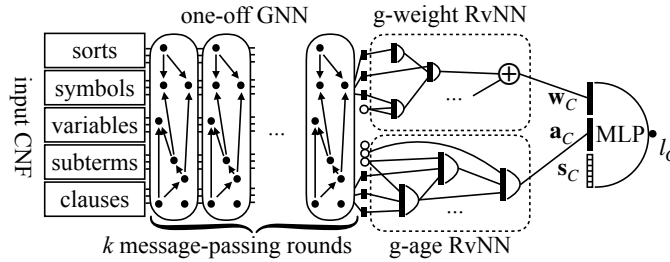


Fig. 2. Clause evaluation neural architecture. Information flows from left to right.

distinct variables and the RvNN produces the same embedding vector for, e.g., both $r(X, Y)$ and $r(Y, X)$). The figure also highlights that a clause embedding here is obtained as a simple sum of its constituent literals’ embeddings.

At the same time, the generalized-age RvNN uses the input-clause embeddings from the GNN and embeds the derived clauses by recursing along the clause derivation history. Fig. 2 shows that each inner node combines the embeddings from the parents and from the used inference rule’s trainable embedding (denoted by the empty circles). Thus it is possible that, e.g., a clause D derived from clauses C_1 and C_2 will obtain a different embedding depending on whether it is derived by the subsumption resolution rule or by the binary resolution rule.

In the very right, Fig. 2 shows the final step of combining the embeddings from the two RvNNs with the simple clause features mentioned earlier and passing them through a fully-connected neural block (MLP). Let us spell out the mathematical details of this final step, because similar operations are also being performed within the GNN and RvNN parts (and were just not detailed here).

Let $n, m \in \mathbb{N}$ be the *embedding size* and the *expanded size* hyper-parameters, respectively. For a clause C , the final MLP receives the generalized weight and age embeddings $\mathbf{w}_C \in \mathbb{R}^n$ and $\mathbf{a}_C \in \mathbb{R}^n$, resp., and C ’s simple features vector $\mathbf{s}_C \in \mathbb{R}^{12}$. The single hidden layer computes

$$\mathbf{h}_C = \text{ReLU}(\mathbf{W}_1 \cdot [\mathbf{w}_C, \mathbf{a}_C, \mathbf{s}_C] + \mathbf{w}_2),$$

an affine transformation with learnable tensors $\mathbf{W}_1 \in \mathbb{R}^{m \times (2n+12)}$ and $\mathbf{w}_2 \in \mathbb{R}^m$ followed by the standard activation function $\text{ReLU}(\mathbf{x}) = \max(\mathbf{0}, \mathbf{x})$. And the final step is the linear $l_c = \mathbf{w}_3^T \cdot \mathbf{h}_C$, for a learnable vector $\mathbf{w}_3 \in \mathbb{R}^m$.¹¹

5 Implementation

We integrated the clause-selection-guiding NN into VAMPIRE 4.9.¹² The prover’s extension relies on PyTorch 2.5 library [27] and the TorchScript bridge for interfacing the neural model trained in Python from C++. Although we initially

¹¹ Further architecture details, in particular the construction of the CNF graph and the computational details of the GNN and the RvNNs have been moved to Appendix B.

¹² <https://github.com/vprover/vampire/releases/tag/mtpa-gnn-cade2025>

aimed this way for zero code duplication between the Python training scripts and the invocation of the network from VAMPIRE, in the end, it was essential for good performance to duplicate the RvNN logic (cf. Sect. 4.1) in C++.¹³

5.1 Single Queue Integration

When running under neural guidance, VAMPIRE relies on a single queue ordered by the clause scores produced by the NN (the logits) to represent the passive set. While properly sampling from the corresponding softmax distribution—as suggested by the theory (cf. Sect. 3.1)—seemed too costly, adding a small amount of noise to the scores once generated, turned out to be a good way to diversify the search and solve additional problems on repeated runs.

Inspired by the Gumbel-max trick [11, 22], we optionally add a Gumbel noise¹⁴ sample g_C to the score of each clause (possibly scaled by a temperature parameter). The nice property this noise has is that

$$\arg \max(\{l_C + g_C\}_{C \in \mathcal{P}}) = \text{softmax}(\{l_C\}_{C \in \mathcal{P}}) \text{ (as distributions),}$$

so except for the fact that the Gumbel offsets g_C are “frozen” (i.e., not drawn fresh for each clause selection round) we achieve exactly the desired effect.

5.2 Delayed Insertion Buffer

To group as many clauses as possible for a single bulk evaluation by the NN (cf. Sect. 4.1) while adhering to a principle that at the time of clause selection all passive clauses must already be assigned a score,¹⁵ we extended VAMPIRE’s passive clause container with a buffer of clauses waiting for evaluation before they can be inserted into the clause selection queue. The buffer is important for the efficient maintenance of the passive set, because often a large fraction of newly derived clauses need not be evaluated and are instead forward-simplified (or deleted through subsumption) or clause splitting triggers changes on the passive set within the AVATAR architecture [40], all before it is necessary to know the clause scores for the next clause selection step.

5.3 Iterative Improvement Loop

We use a collection of Python scripts to orchestrate 1) running VAMPIRE to collect performance data, 2) rerunning the successful proof attempts in a mode that collects traces,¹⁶ and 3) feeding these traces to our RL-inspired learning

¹³ Relying on LibTorch, the C++ distribution of PyTorch.

¹⁴ Can be computed as $g = -\log(-\log(u))$ when sampling $u \sim \text{Uniform}(0, 1)$.

¹⁵ Related work [13] explored postponing the evaluation of newly derived clauses until there is a certain number of them. This, however, may lead to the selection of a suboptimal clause while the current best clause is still waiting to be evaluated.

¹⁶ This incurs a performance penalty so unlike step 1) is run without a strict time limit. We made sure there is no non-determinism that would prevent reliable reproduction.

operator (cf. Sect. 3.1) to improve the guiding NN, all in a potentially infinite loop. We use parallel processing to speed these operations as much as possible when run on a machine with multiple CPUs (but do not make use of GPUs).

We make one noteworthy departure from RL practices in step 3). Instead of performing just one gradient descent step in each loop (as REINFORCE would), we always separate a random 20% of the available traces for validation purposes and have an inner loop of training rounds use the remaining 80% of the traces to repeat gradient descent until the validation loss¹⁷ does not improve (for 5 successive rounds). This is a standard *early stopping* regularization criterion known from supervised learning, which in our case greatly accelerates convergence.¹⁸

6 Experiments

We use the TPTP library [38] v9.0.0 for our experiments. TPTP is very diverse, containing problems from many domains and of various encodings collected over several decades from many sources. This poses a challenge for ML-based guiding methods as there are likely no immediate broad commonalities across the problems the learning could capitalize on. Indeed, very few successes with improving ATPs via learning have been reported in the literature for this library to date.

The first-order subset of the library consists of 19 477 problems and we randomly split those into 15 000 training problems and the rest, left for independent testing. For the main set of experiments we used an instruction limit¹⁹ of 30 000 Mi per proof attempt, which amounts on average to 10.4s of wall clock time on our servers.²⁰ Unless stated otherwise, we fixed the NN parameters to: embedding size $n = 32$, expanded size $m = 256$, and $k = 8$ GNN rounds. With these parameters, the neural model takes up a bit less than 1.6 MB of disk space.

We use VAMPIRE’s *default strategy* both as the source of initial training traces (relying on the default clause selection heuristic, 1:1 age-weight alternation), as well as the basis for the neurally guided extension (with clause selection guided by the NN; cf. Sect. 5.1). The default strategy employs the AVATAR architecture [40] and the limited resource strategy (LRS), a version of the Otter saturation loop with a preemptive clause removal determined by an estimation of the speed of clause processing and the approaching time (instruction) limit [28]. Since delayed evaluation (cf. Sect. 5.2) is in conflict with timely LRS estimations and eager evaluation by the relatively expensive NN did not make LRS pay off anymore, we disabled LRS in the neurally guided version.

¹⁷ Strictly speaking, Sect. 3.1 describes gradient *ascent* with no explicitly loss. However, the role of a loss for gradient descent is in our case played by the expression $-\delta$ if understood “before the gradient operator is applied.”

¹⁸ The single-step and iterated approach actually converge to the same fixed point [10].

¹⁹ Instruction limiting leads to more robust results than time limiting in situation (like ours) where many processes compete for the main memory (cf. Appendix A of [35]).

²⁰ Equipped with AMD EPYC 7513 (128 cores with 2.6 GHz) and 500 GB RAM.

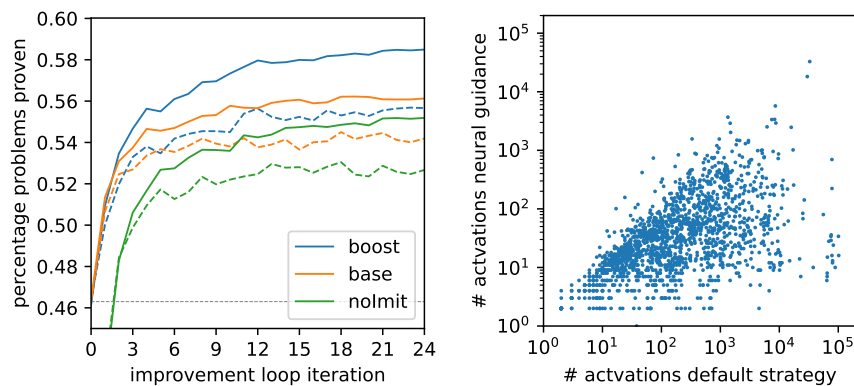


Fig. 3. Left: performance progress of three selected training sessions (test performance dashed). Right: scatter plot comparing the number of clause activations needed by the default and the neurally guided strategies, resp., on commonly solved test problems.

Base experiment. The default strategy solves approximately 46.3% (6940) of the training problems. Fig. 3 (left; *base*) shows the iterative improvement process progressing from this baseline level (marked by the horizontal gray line) to 56.2% training problems solved after 24 iterations.²¹ At the same time, the test performance maxes with 54.5%, which means a 17.8% improvement over the baseline. This shows that the trained model generalizes well from the training experience and enables VAMPIRE to solve many new problems.²²

Neural Guidance Cost and Quality. Around one third of the 30 000 Mi allotted instructions (measured over unsuccessful runs that make it past parsing and preprocessing) is on average spent by the NN: 470 Mi to load a model from the disc, 1740 Mi by the GNN computation, and 9420 Mi on evaluating clauses during saturation. To compensate for this overhead, the trained model offers a clause selection heuristic that is very precise. In Fig. 3 (right) the neurally guided strategy needs on average 5.5-times fewer activations than the default one and in only 7.2% of the cases it needs more activations to solve a given problem.

“Without Imitation.” In addition to the base experiment, two other training sessions have their improvement progress shown in Fig. 3 (left). The *nolmit* experiment starts the first loop iteration from a randomly initialized network (rather than the default strategy) to generate the first set of traces. While this is arguably more a property of the TPTP library²³ than of the training method, it

²¹ The experiment took approximately 24 hours to complete, when utilising 120 cores for the prover evaluation and trace collection and 60 cores for the training.

²² Several other experiments and technical details appear in Appendix C.

²³ In that it contains enough problems so easy that even an essentially random clause selection heuristics is able to solve them, yet sufficiently non-trivial ones that the corresponding solution traces can serve as a basis for subsequent improvement.

is interesting to see that the baseline can be improved upon even without imitating the default clause selection heuristic. However, the lower final performance suggests that the missing additional examples impair generalization.

Boost. The training session labeled in Fig. 3 (left) boost led to our current strongest guiding NN trained from the 30 000 Mi-limited runs. It improves in test performance by 20% over the baseline. The boost session relies on using several repeated runs of the prover to collect more training traces in each iteration,²⁴ and, additionally, assigns more weight in the training to (traces from) problems solved only in recent loop iterations, while the weight of problems solved repeatedly in past successive loops is gradually decreased.²⁵

Solving Hard Problems. To check whether our neural guidance can also help VAMPIRE solve hard problems, we ran one more training session, but this time with runs limited at 100 000 Mi (~ 39.0 s) on the whole first-order TPTP. Note that not using a train/test split is fine here, because none of the problems we now report were solved by the seeding default strategy and so they had to be attained solely thanks to generalization. During the 30 improvement loops for which this experiment ran,²⁶ it solved 130 TPTP problems of rating 1.0.

A problem of TPTP rating 1.0 has the property that no known system was able to solve it during the last rating evaluation [38]. However, there are many rating 1.0 problems that had a rating smaller than 1.0 in the past. Out of our 130 problems, we found 49 that were actually never solved even once in the past.²⁷ This is a remarkable occurrence in the context of a single strategy improvement.

Put Into Perspective. We close this section with a *cactus plot* of Fig. 4, which shows the cumulative performance of several strategies as a function of time. First to notice is that the two neurally-guided strategies, `boost(all100K)` and `boost(30k)`, start solving any problems only after the 1000 Mi mark, which is caused by the non-trivial start-up time of the guiding NN. `boost(all100K)` is the strategy presented in the previous paragraph and, as noted, has been trained also on the testing split of our problems; as such it does not constitute a fair comparison and is included only to provide a perspective. The default strategy is shown in 4 variants: `default`, `otter` (which means turning off the LRS trick), a conjecture-directed variant (`nwc=5`)²⁸ and a variant with AVATAR turned off.

²⁴ Instead of one run, we use 5 independently seeded runs with VAMPIRE’s input and internal shuffling [36] enabled and for the neurally guided runs we also add the Gumbel noise to the logits (cf. Sect. 5.1) with temperatures $\tau \in \{0, 1/27, 1/9, 1/3, 1\}$.

²⁵ Giving different weights to problems depending how useful they seem for the training appears to be a neat trick we plan to explore more thoroughly in future work.

²⁶ Taking 12.4 days to complete, while using 64 cores for the prover evaluation and trace collection and 32 cores for training.

²⁷ And 8 that had UNK status, so that it was not known until now whether they can be proven, or whether their conjecture is, in fact, false.

²⁸ NWC stands for “non-goal weight coefficient” and means that any clause not derived from the conjecture will have its standard clause selection weight multiplied by 5.

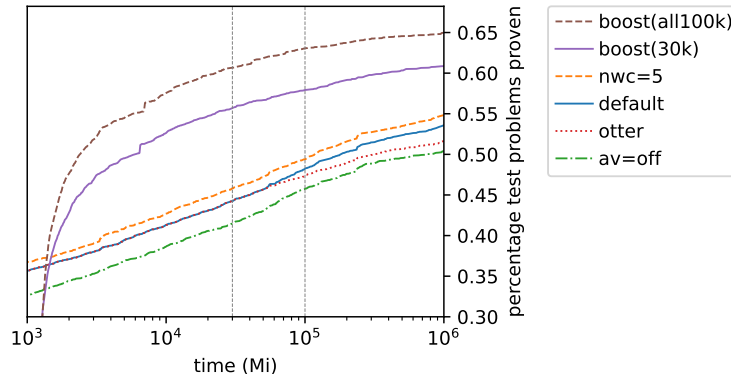


Fig. 4. Test performance cactus plot for VAMPIRE’s default strategy (and three variants) and two neurally guided strategies. (Vertical lines at 30 000 Mi and 100 000 Mi.)

We would like draw the attention to the relative sizes of the jump in performance between `av=off` and `default` and between `default` and `boost(30k)`. When introduced, AVATAR came about as a major improvement in VAMPIRE’s performance, now we can see a much larger jump thanks to our neural guidance.

7 Related Work

The area of machine learning for theorem proving has been developing at a rapid pace in recent years [4]. Let us, therefore, focus here only on the most related approaches, those targeting the clause selection heuristic in saturation-based theorem proving.

Of these a prominent role is played by ENIGMA [14, 6, 13] and systems inspired by it [21, 33, 34]. Setting aside the ML technology used for now, we can single out a common *ENIGMA-style learning operator* and compare it to the one proposed in this work. While both approaches learn from successful prover runs and rely on proof clauses as their source of positive examples, ENIGMA only uses the recorded selected clauses to form the negative background (as opposed to the typically much larger set of generated clauses used here), and, moreover, it puts these clauses onto one pile, abstracting away the flow of time (while the RL-inspired operator uses each clause selection moment in the trace as an independent situation to learn from).²⁹ ENIGMA can be seen to already assume a reasonably strong clause selection heuristic and mainly seeks to improve upon it through the integration of the learned guidance. This is reflected in the observation that ENIGMA works best when combined with the baseline clause selection heuristic in some way (a.k.a. the “coop” mode), while the RL-inspired operator aims to provide independent guidance backed by a single clause

²⁹ Chvalovský et al. [7] (Sect. 6.2) name this distinction *classic vs dynamic* data and also prefer the latter for the training, as it is closer to the situation at inference time.

selection queue. Interestingly, while ENIGMA trains a binary classifier whereas the RL-inspired operator relies on the policy gradient theorem, the resulting formula for gradient descent is essentially the same (negative log likelihood).

Among RL approaches, TRAIL [1] also derives its loss from policy gradient, but distinguishes itself by employing an attention mechanism to capture dependencies on the evolving state. McKeown and Sutcliffe [24] use a value-based method, but only aim to learn a meta-heuristic: an agent who picks which queue, out of the many provided by E prover [30], to selected the next clause from.

Regarding neural architectures, the use of a GNN is not novel in our context [26, 13, 1], but the listed approaches apply it both to the input problem as well as to the derived clauses. NIAGRA [9], a successor of TRAIL, similarly to our approach, uses a start-up invocation of a GNN of the (often large) input problem to prepare symbol embeddings to later use cheaply during saturation. Embedding of formula syntax using RvNNs was historically the first use-case of the technology [20], but more recently appeared, e.g., in ENIGMA-NG [6]. An RvNN unrolling along clause derivation history comes from Deepire [33, 34].

8 Conclusion

We proposed a new neural architecture for clause selection guidance in an ATP and a learning operator for its iterative improvement inspired by RL. The architecture integrates a start-up GNN with two RvNNs, ensuring name invariance, efficiency in evaluation and strong performance thanks to access to both the clause’s syntax as well as to its derivation history. The learning operator assumes no evolving state as it suggests learning a single score pre clause, but draws experience independently from all the possibly many snapshots of the passive set along a successful proof attempt’s trace. The resulting neural clause selection heuristic is implemented as a single standalone clause selection queue.

On problems from the TPTP library, a particularly challenging benchmark for ML-based methods due to its diverse nature, our new neural guidance improves the performance of VAMPIRE’s default strategy by 20% and, moreover, allows the prover to solve many problems not previously tackled by any known ATP. To the best of our knowledge, this is a first published report of a substantial improvement by ML-based clause selection guidance on the TPTP benchmark.³⁰

There are several interesting directions for future research. One of them is to experimentally compare the relative strengths of the ENIGMA-style and RL-inspired learning operators. Another is the question of transfer learning: Would guidance trained on the TPTP enable VAMPIRE to solve, e.g., more Mizar40 problems (or vice versa)? Most importantly, we are curious about the potential of the new technology for improving whole sets of theorem proving strategies and the corresponding impact on building strong strategy schedules [3], as this is the ultimate measure of an improvement’s impact on the ATP users.

³⁰ In 2020 at CASC-J10, ENIGMA Anonymous [13] improved over E prover, on which it is built, by 50 problems. The details of the success, however, remain unpublished.

Bibliography

- [1] Abdelaziz, I., Crouse, M., Makni, B., Austel, V., Cornelio, C., Ikbal, S., Kapaniathi, P., Makondo, N., Srinivas, K., Witbrock, M., Fokoue, A.: Learning to guide a saturation-based theorem prover. *IEEE Trans. Pattern Anal. Mach. Intell.* **45**(1), 738–751 (2023)
- [2] Ba, L.J., Kiros, J.R., Hinton, G.E.: Layer normalization. *CoRR abs/1607.06450* (2016)
- [3] Bártek, F., Chvalovský, K., Suda, M.: Regularization in spider-style strategy discovery and schedule construction. In: *IJCAR 2024*. LNCS, vol. 14739, pp. 194–213. Springer (2024)
- [4] Blaauwbroek, L., Cerna, D.M., Gauthier, T., Jakubův, J., Kaliszky, C., Suda, M., Urban, J.: Learning guided automated reasoning: A brief survey. In: *Logics and Type Systems in Theory and Practice - Essays Dedicated to Herman Geuvers on The Occasion of His 60th Birthday*. LNCS, vol. 14560, pp. 54–83. Springer (2024)
- [5] Chvalovský, K., Jakubův, J., Olšák, M., Urban, J.: Learning theorem proving components. In: *TABLEAUX 2021*. LNCS, vol. 12842, pp. 266–278. Springer (2021)
- [6] Chvalovský, K., Jakubův, J., Suda, M., Urban, J.: ENIGMA-NG: efficient neural and gradient-boosted inference guidance for E. In: *CADE 2019*. LNCS, vol. 11716, pp. 197–215. Springer (2019)
- [7] Chvalovský, K., Korovin, K., Piepenbrock, J., Urban, J.: Guiding an instantiation prover with graph neural networks. In: *LPAR 2023*. EPiC Series in Computing, vol. 94, pp. 112–123. EasyChair (2023)
- [8] Duarte, A., Korovin, K.: Implementing superposition in iProver. In: *IJCAR 2020*. LNCS, vol. 12167, pp. 388–397. Springer (2020)
- [9] Fokoue, A., Abdelaziz, I., Crouse, M., Ikbal, S., Kishimoto, A., Lima, G., Makondo, N., Marinescu, R.: An ensemble approach for automated theorem proving based on efficient name invariant graph neural representations. In: *IJCAI 2023*. pp. 3221–3229. ijcai.org (2023)
- [10] Ghosh, D., Machado, M.C., Roux, N.L.: An operator view of policy gradient methods. In: *NeurIPS 2020* (2020)
- [11] Gumbel, E.: *Statistical Theory of Extreme Values and Some Practical Applications: A Series of Lectures*. Applied mathematics series, U.S. Government Printing Office (1954)
- [12] Hamilton, W.L., Ying, Z., Leskovec, J.: Inductive representation learning on large graphs. In: *NIPS 2017*. pp. 1024–1034 (2017)
- [13] Jakubův, J., Chvalovský, K., Olšák, M., Piotrowski, B., Suda, M., Urban, J.: ENIGMA Anonymous: Symbol-independent inference guiding machine. In: *IJCAR 2020*. LNCS, vol. 12167, pp. 448–463. Springer (2020)
- [14] Jakubův, J., Urban, J.: ENIGMA: efficient learning-based inference guiding machine. In: *CICM 2017*. LNCS, vol. 10383, pp. 292–302. Springer (2017)

- [15] Jakubův, J., Urban, J.: Hammering Mizar by learning clause guidance (short paper). In: ITP 2019. LIPIcs, vol. 141, pp. 34:1–34:8. Schloss Dagstuhl - Leibniz-Zentrum für Informatik (2019)
- [16] Kaliszyk, C., Urban, J.: Mizar 40 for mizar 40. *J. Autom. Reason.* **55**(3), 245–256 (2015)
- [17] Kaliszyk, C., Urban, J., Michalewski, H., Olšák, M.: Reinforcement learning of theorem proving. In: NeurIPS 2018. pp. 8836–8847 (2018)
- [18] Kocsis, L., Szepesvári, C.: Bandit based monte-carlo planning. In: ECML 2006. LNCS, vol. 4212, pp. 282–293. Springer (2006)
- [19] Kovács, L., Voronkov, A.: First-order theorem proving and Vampire. In: CAV 2013. LNCS, vol. 8044, pp. 1–35. Springer (2013)
- [20] Küchler, A., Goller, C.: Inductive learning in symbolic domains using structure-driven recurrent neural networks. In: KI 1996. LNCS, vol. 1137, pp. 183–197. Springer (1996)
- [21] Loos, S.M., Irving, G., Szegedy, C., Kaliszyk, C.: Deep network guided proof search. In: LPAR 2017. EPiC Series in Computing, vol. 46, pp. 85–105. EasyChair (2017)
- [22] Maddison, C.J., Tarlow, D., Minka, T.: A* sampling. In: NIPS 2014. pp. 3086–3094 (2014)
- [23] McCune, W.: OTTER 3.3 reference manual. CoRR **cs.SC/0310056** (2003), <http://arxiv.org/abs/cs/0310056>
- [24] McKeown, J., Sutcliffe, G.: Reinforcement learning for guiding the E theorem prover. In: FLAIRS 2023. AAAI Press (2023)
- [25] Mnih, V., Kavukcuoglu, K., Silver, D., Graves, A., Antonoglou, I., Wierstra, D., Riedmiller, M.A.: Playing Atari with deep reinforcement learning. CoRR **abs/1312.5602** (2013)
- [26] Olšák, M., Kaliszyk, C., Urban, J.: Property invariant embedding for automated reasoning. In: ECAI 2020. Frontiers in Artificial Intelligence and Applications, vol. 325, pp. 1395–1402. IOS Press (2020)
- [27] Paszke, A., Gross, S., Massa, F., Lerer, A., Bradbury, J., Chanan, G., Killeen, T., Lin, Z., Gimelshein, N., Antiga, L., Desmaison, A., Kopf, A., Yang, E., DeVito, Z., Raison, M., Tejani, A., Chilamkurthy, S., Steiner, B., Fang, L., Bai, J., Chintala, S.: Pytorch: An imperative style, high-performance deep learning library. In: Advances in Neural Information Processing Systems 32, pp. 8024–8035. Curran Associates, Inc. (2019)
- [28] Riazanov, A., Voronkov, A.: Limited resource strategy in resolution theorem proving. *J. Symb. Comput.* **36**(1-2), 101–115 (2003)
- [29] Schulman, J., Wolski, F., Dhariwal, P., Radford, A., Klimov, O.: Proximal policy optimization algorithms. CoRR **abs/1707.06347** (2017)
- [30] Schulz, S., Cruanes, S., Vukmirovic, P.: Faster, higher, stronger: E 2.3. In: CADE 2019. LNCS, vol. 11716, pp. 495–507. Springer (2019)
- [31] Schulz, S., Möhrmann, M.: Performance of clause selection heuristics for saturation-based theorem proving. In: IJCAR 2016. LNCS, vol. 9706, pp. 330–345. Springer (2016)
- [32] Silver, D., Hubert, T., Schrittwieser, J., Antonoglou, I., Lai, M., Guez, A., Lanctot, M., Sifre, L., Kumaran, D., Graepel, T., Lillicrap, T., Simonyan,

- K., Hassabis, D.: A general reinforcement learning algorithm that masters chess, shogi, and Go through self-play. *Science* **362**(6419), 1140–1144 (2018)
- [33] Suda, M.: Improving ENIGMA-style clause selection while learning from history. In: CADE 2021. LNCS, vol. 12699, pp. 543–561. Springer (2021)
- [34] Suda, M.: Vampire with a brain is a good ITP hammer. In: FroCoS 2021. LNCS, vol. 12941, pp. 192–209. Springer (2021)
- [35] Suda, M.: Vampire getting noisy: Will random bits help conquer chaos? EasyChair Preprint no. 7719 (2022), <https://easychair.org/publications/preprint/CSVF>
- [36] Suda, M.: Vampire getting noisy: Will random bits help conquer chaos? In: IJCAR 2022. LNCS, vol. 13385, pp. 659–667. Springer (2022)
- [37] Sutcliffe, G.: The CADE ATP System Competition – CASC. *AI Magazine* **37**(2), 99–101 (2016)
- [38] Sutcliffe, G.: Stepping Stones in the TPTP World. In: IJCAR 2024. pp. 30–50. No. 14739 in LNAI (2024)
- [39] Sutton, R.S., Barto, A.G.: Reinforcement Learning: An Introduction. A Bradford Book, Cambridge, MA, USA (2018)
- [40] Voronkov, A.: AVATAR: the architecture for first-order theorem provers. In: CAV 2014. LNCS, vol. 8559, pp. 696–710. Springer (2014)
- [41] Weidenbach, C., Dimova, D., Fietzke, A., Kumar, R., Suda, M., Wischniewski, P.: SPASS version 3.5. In: CADE 2009. LNCS, vol. 5663, pp. 140–145. Springer (2009)
- [42] Williams, R.J.: Simple statistical gradient-following algorithms for connectionist reinforcement learning. *Mach. Learn.* **8**, 229–256 (1992)
- [43] Zombori, Z., Urban, J., Olšák, M.: The role of entropy in guiding a connection prover. In: TABLEAUX 2021. LNCS, vol. 12842, pp. 218–235. Springer (2021)

A List of the Used Simple Clause Features

Table 1. Simple features of clause C . The domains \mathbb{N} and \mathbb{B} are only conceptual and get converted to \mathbb{R} in the obvious way.

short name	domain	description
age	\mathbb{N}	depth of C 's derivation tree (only counting generating inferences)
weight	\mathbb{N}	number of symbol occurrences in C
posLen	\mathbb{N}	number of positive literals in C
negLen	\mathbb{N}	number of negative literals in C
justEq	\mathbb{B}	Are all literals equational?
justNeq	\mathbb{B}	Are all literals non-equational?
numVarOcc	\mathbb{N}	Number of variable occurrences in C
numVarOccNorm	$\mathbb{R}^{[0,1]}$	$\text{numVarOcc}(C) / \text{weight}(C)$
fromGoal	\mathbb{B}	Does C have a conjecture clause as an ancestor?
sineMaxed	\mathbb{B}	SInE fix point computation did not reach C at all?
sineLevelNorm	$\mathbb{R}^{[0,1]}$	if sineMaxed(C) then 1.0 else $0.5 \times (\text{sineLevel}(C) / \text{maxSineLevelAssigned})$
numSplits	\mathbb{N}	number of AVATAR assumptions that C depends on

B Further Architecture Details

CNF Graph. As mentioned, the graph corresponding to the input CNF has five kinds of nodes: sort, symbol, variable, subterm, and clause nodes. It also has 8 distinct kinds of edges. (For the GNN message passing, though, opposite edges to each kind are added too, so there are in total 16 convolution kernels in each message passing round.) Each node kind comes with a set of features to distinguish the individual nodes, if possible.

For an unsorted FOL problem, we introduce two sort nodes: \$i (default) and \$o (boolean), where \$o is used as an output sort of predicate symbols. In a multi-sorted problem, user-defined sorts are added; in a problem with arithmetic we also add \$int, \$rat, or \$real, as needed. Sort nodes are represented by a feature vector of length 3, with Boolean features ‘isPlain’, ‘isBoolean’, and ‘isArithmetic’.

Symbols are both the predicate symbols and the function symbols. We use 10 features for symbols: isEquality, isFunctionSymbol, isIntroduced (introduced by VAMPIRE during preprocessing), isSkolem (skolems are introduced, but there are other introduced symbols than skolems), isInterpretedNumber (such as 1 of sort \$int, 2.0 of sort \$real, etc.), and arityGreaterThanX, where $X \in \{0, 1, 2, 4, 8\}$.

There is an edge (kind 1) from each symbol node to the symbol’s output sort node. There are also edges (kind 2) from symbols to larger symbols in the precedence. These form a linear chain between the immediate neighbours, but

also regular jumps of length $2^i, i > 0$, so that in total not more than $n \log n$ edges are added. These ordering edges are added separately for the predicate symbol and function symbol nodes. We have not yet checked whether these edges meaningfully increase the expressive power of the GNN.

Variable, subterm and clause nodes are introduced together. They reflect the actual syntactic material of the input CNF, but unlike the processing in the RvNNs, these are *not shared* (allowing the latent meanings to be clause-local).

Variable nodes are created for the variables of each clause separately. A clause $C = p(X, Y) \vee q(X)$ has two variables, X and Y , so it causes two variable nodes to be added. Variable nodes have a single feature, an ordinal number of that variable as it was encountered during the processing of its clause. So if we add variable nodes v_X and v_Y for the sake of clause C , the node v_X will get feature 0 and v_Y feature 1 or vice versa. A variable node is connected to its clause’s node by an edge (kind 3) and to its sort’s node by another one (kind 4).

Subterm nodes are either literal nodes or proper subterm nodes, all the way down to terminal subterms: constant occurrences (function symbols of arity 0 applied to their 0 arguments) and variable occurrences. Each variable-occurrence node as a subterm node has an edge to a variable node (kind 5) of its variable. Each non-variable-occurrence node has an edge (kind 6) to its functor’s symbol node. Obviously, subterm nodes are connected by edges (kind 7) reflecting the immediate subterm relation. Subterm nodes are represented by the following 10 features: literalSign (either 1 or -1 for literal subterms, 0 for proper subterms), positionUnderParent (0 for literal subterms, linearly interpolating between 0.0 and 1.0 for proper subterms, e.g., in $p(a, b, c)$ this feature would be 0.0 for a , 0.5 for b and 1.0 for c), numVariableOccurrencesGreaterThan X for $X \in \{0, 2, 4, 8\}$ and weightGreaterThan Y for $Y \in \{1, 4, 16, 64\}$.

Clause nodes are connected by an edge (kind 8) to their literals’ subterm nodes. Each clause is represented by the following 10 features: isDerivedFromGoal, isTheoryAxiom, hasSizeGreaterThan X for $X \in \{1, 2, 4, 8\}$ (i.e., the number of literals) and hasWeightGreaterThan Y for $Y \in \{4, 16, 64, 256\}$.

GNN Computation. For each of the five node kinds, we first pass the node feature matrix through a dedicated learnable affine transformation to obtain an initial embeddings of size n and apply the ReLU non-linearity.

In each of the k message-passing rounds that follow, GraphSAGE convolutions [12] are used to pass messages along each edge kind ξ . This means that new node embedding contributions \mathbf{x}^ξ are computed from the old embeddings \mathbf{x} via

$$\mathbf{x}_i^\xi = \mathbf{W}_1^\xi \mathbf{x}_i + \mathbf{W}_2^\xi \cdot \text{mean}_{j \in \mathcal{N}^\xi(i)} \mathbf{x}_j,$$

where $\mathcal{N}^\xi(i)$ are the nodes with an edge of kind ξ leading to node i .

The overall new node embeddings \mathbf{x}' are obtained by summing the contributions \mathbf{x}^ξ over all edge kinds ξ whose target node kind we are just discussing. For example, the embeddings for sorts receive (and sum up) contributions from symbols (along edge kind 1) and variables (along edge kind 4). Then the non-linearity ReLU is applied to the new node embeddings \mathbf{x}' , they replace old node

embeddings \mathbf{x} and the process can be repeated. We stress that in each such message-passing round the convolution kernels (i.e., the matrices \mathbf{W}_1^ξ and \mathbf{W}_2^ξ) are different (we omitted the round index not to clutter the notation).³¹

As a final step, there is another set of learnable affine transformations applied 1) to the GNN clause embeddings, to promote them to the generalized-age RvNN initial clause embeddings, and 2) to the GNN symbol embeddings, to promote them to the generalized-weight RvNN symbol embeddings.

RvNN Computation. The generalized-age RvNN uses a matrix of trainable embeddings of the inference rules $\mathbf{W}^{inf} \in \mathbb{R}^{n \times r}$, where $r = 205$ is the number of distinct inference rules recognized by VAMPIRE.³² Its recursive step (the “combine” operation) is a single-hidden-layer MLP (similar to the final step already explained) and computes, for a clause C derived by inference rule i from n_p parents with already computed generalized-age embeddings $\mathbf{p}_C^1, \dots, \mathbf{p}_C^{n_p}$,

$$\mathbf{h}_C^a = \text{ReLU}(\mathbf{W}_1^a \cdot [\mathbf{W}^{inf} \cdot e_i, \mathbf{p}_C^1, \text{mean}_{k=2}^{n_p} \mathbf{p}_C^k] + \mathbf{w}_2^a),$$

where $\mathbf{W}_1^a \in \mathbb{R}^{m \times 3n}$, $\mathbf{w}_2^a \in \mathbb{R}^m$ and the expression in the square bracket denotes a concatenation of 1) the i -th rule embedding, 2) the first parent embedding, and 3) the averaged remaining parent embeddings (as already mentioned at the end of Sect. 4.1). One additional affine transformation completes the generalized-age embedding of clause C via

$$\mathbf{a}_C = \text{LayerNorm}(\mathbf{W}_3^a \cdot \mathbf{h}_C^a + \mathbf{w}_4^a),$$

where $\mathbf{W}_3^a \in \mathbb{R}^{n \times m}$, $\mathbf{w}_4^a \in \mathbb{R}^n$ and LayerNorm is the layer normalization step [2], important for the stability of training involving many nested recursion steps.

The generalized-weight RvNN recursive step is analogous in many respects. There is a single variable subterm embedding $\mathbf{w}^{var} \in \mathbb{R}^n$ retrieved when an argument subterm is a variable. We also use a single real number to encode the polarity p of each subterm, similarly to how it is done in the GNN (i.e., proper subterms have $p = 0$, positive literals $p = 1$ and negative literals $p = -1$). So, assuming a term t to embed has functor f with a symbol embedding $\mathbf{s}_f \in \mathbb{R}^n$, polarity $p \in \mathbb{R}$, and k already embedded argument subterms s_1, \dots, s_k (some of which may be variables) with respective embeddings $\mathbf{s}_1, \dots, \mathbf{s}_k$, we first compute

$$\mathbf{h}_t^w = \text{ReLU}(\mathbf{W}_1^w \cdot [\mathbf{s}_f, p, \mathbf{s}_1, \text{mean}_{j=2}^k \mathbf{s}_j] + \mathbf{w}_2^w),$$

with $\mathbf{W}_1^w \in \mathbb{R}^{m \times 3n+1}$, $\mathbf{w}_2^w \in \mathbb{R}^m$, replacing \mathbf{s}_1 with $\mathbf{0} \in \mathbb{R}^n$ whenever $k = 0$, and follow it up with

$$\mathbf{t} = \text{LayerNorm}(\mathbf{W}_3^w \cdot \mathbf{h}_t^w + \mathbf{w}_4^w),$$

³¹ The intuition is that in each round the level of abstraction at which the data is internally represented may be shifting, from the rudimentary features we provide at the beginning, towards more high-level concepts that reflect the CNF more globally.

³² While only a small subset of these rules is actually utilized by the default strategy used in our experiments, it is convenient to allocate the full table and index the rules by their native id as obtained from the prover’s source code.

with $\mathbf{W}_3^w \in \mathbb{R}^{n \times m}$, $\mathbf{w}_4^w \in \mathbb{R}^n$. As mentioned, the generalized-weight embedding of a clause $C = L_1 \vee \dots \vee L_k$ is computed simply as the sum

$$\mathbf{w}_C = \sum_{i=1}^k \mathbf{l}_i,$$

with \mathbf{l}_i standing for the subterms embeddings of the respective literals L_i .

C Architecture and Training Setup Ablations

In addition to the hyper-parameters mentioned in the main text, we used a base learning rate $\alpha = 0.0002$, which decayed exponentially with each improvement iteration by a factor of 0.87055, i.e., halving every five iterations.

Unlike in the main text, all experiments reported here used an instruction limit of 10 000 Mi and, for the GNN, $k = 10$ message passing rounds by default.

Adaptive Problem Weights. In addition, all experiments reported here applied the adaptive problem weighting scheme (mentioned in the main text as part of the `boost` session). In more detail, the scheme works as follows.

Given basic hyper-parameters $maxStrength = 2.0$ and $staleAfter = 5$ and a derived parameter

$$base = maxStrength^{\frac{1}{2 * staleAfter}},$$

each solved problem P maintains its score initialized to $score_P = 0$. The idea is that a relative weight of the problem’s trace(s) in the overall loss expression is $base_P^{score}$, i.e., starting at 1, and that $score_P$ is updated as follows. Each iteration in which the problem is solved, its score is decreased by 1, each time it is not solved, its score is increased by 2. However, if it is not solved for $staleAfter$ successive iterations, the problem is declared “stale” and is not learned from anymore. The overall intuition is that easy problems should contribute less than those the current version of the guidance struggles with.

In a particular improvement session (referred to as `base10k` below), the seeding default strategy solved 6529 problems, which gave rise to 5560 traces to learn from (really easy problems are solved without requiring any clause selection steps and cannot be learned from). After 30 iterations, 4999 problems ended up with the lowest possible score -29 and more than a thousand additional problems were assigned score from $\{-28, -27, -26\}$. A maximal final score was 34, for a problem that necessarily alternated between being solved and not being solved through consecutive iterations several times.

NN Architecture Building Blocks. Fig. 5 shows an analogue of Fig. 3 (left), plotting the iterative improvement progress for variants of our architecture without one or two of its key building blocks: the generalized-age RvNN, the generalized-weight RvNN, and the simple features. We see that combining all three is the best, but each one can be dropped without sacrificing the performance too much. On the other hand, a single building block alone is always much worse, and the

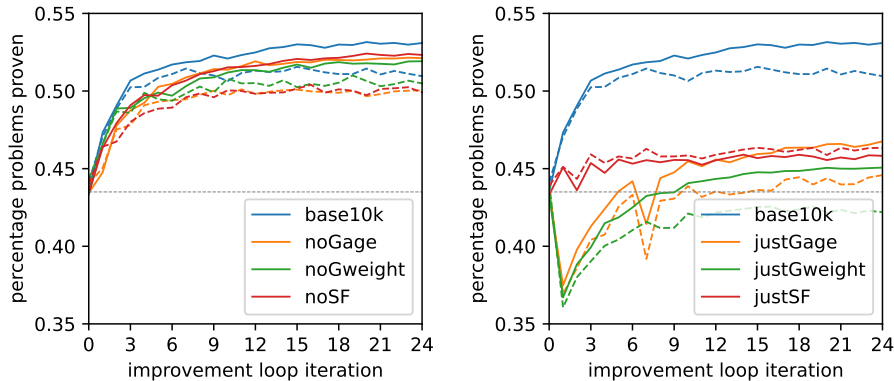


Fig. 5. Performance progress for variants of our NN architecture with a single building block disabled (left) and a single block enabled (right), compared to the same baseline (**base10k**) which includes the blocks. **Gage** means the generalized-age RvNN, **Gweight** the generalized-weight RvNN and **SF** stands for the simple features.

RvNNs alone cannot even improve over the baseline after the first iteration of improvement. Interestingly, only using generalized weight for the guidance ends up being worse than only using generalized age. Simple features alone are relatively easy to learn and their test performance is actually greater than their train performance here, suggesting (not surprisingly) a very low tendency to overfit.

NN Size Parameters. Fig. 6 shows the performance of our architecture when varying the embedding size and the expanded size hyper-parameters (left), and the number of GNN message passing rounds (right). We can see that regarding the first two, at least in the range experimented with, bigger is always better: Reducing the embedding size to $n = 16$ impairs performance noticeably, reducing the expanded size to $m = 128$ a bit less, and increasing the embedding size to $n = 48$ seems potentially even slightly better than the default in test performance and comparable in train performance. The main reason why we did not use larger values in the main experiment was the increased memory requirement of the training procedure, for which 60 parallel training processes would threaten not to fit into the available 0.5TB of RAM at peak consumption moments.

On the other hand, the value $k = 8$ of GNN message passing round was in our setting at an upper end of the range of favorable values. We see that $k = 4$ works comparably well, and $k = 16$ is definitely worse. An separate investigation revealed that the latter is mainly not due to the extra time required to process the GNN layers at startup, but rather due to reduced ability to generalize.

The discussed hyper-parameters influence the number of trainable parameters of the network (i.e., $|\theta|$), which is reflected by the corresponding file size of the model on the disk. Table 2 shows the file sizes for the models from Fig. 6.

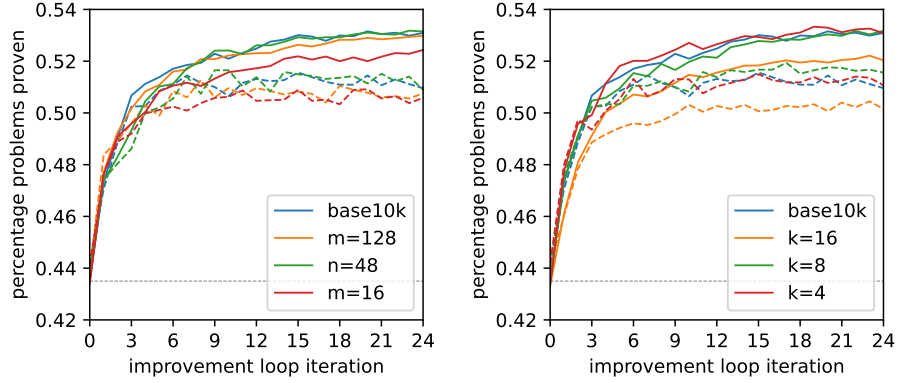


Fig. 6. Performance progress for variants of NN of different embedding size (n) and expanded size (m) (left), and different number of GNN message passing rounds (k) (right). Recall that `base10k` uses $n = 32$, $m = 256$, and $k = 10$.

Table 2. Model file sizes as function of hyper-parameters n , m , and k .

session name	n	m	k	file size
base10k	32	256	10	1.9 MB
n=48	48			3.6 MB
n=16	16			0.8 MB
m=128		128		1.7 MB
k=4			4	1.0 MB
k=8			8	1.6 MB
k=16			16	2.8 MB